The Experimental Hygrothermal Performance of a Robust Cold-Climate Retrofit Interior Foundation Wall Insulation System

Louise F. Goldberg, PhD **Mark L. Stender**

ABSTRACT

A durable interior foundation wall retrofit insulation system, including a water management system in compliance with the foundation wall performance option in the 2009 Minnesota Energy Code*, has been developed, patented, and tested. The system was tested in an interior foundation wall insulation retrofit application on a masonry block foundation wall using two different types of interior insulation. An interior basement insulation system without a water management system was used as a control. The system was tested under a severe internal boundary condition regime in which the relative humidity reached a maximum value of 72% during the heating season. During the cooling season, water was injected into the system via a spray bar to mimic bulk water leakage through the foundation wall. The results confirm that the water management system was effective in draining bulk water and condensate from both sides of the water separation plane in compliance with the requirements of the performance option under the imposed severe boundary conditions.*

INTRODUCTION

A core difficulty in designing durable interior basement wall insulation systems in cold climates (Department of Energy Climate Zones 6 and 7 [ICC 2006]) is the management of bulk water generated on the condensing planes of the insulation system. The condensate is generated from interior-, soil-, and ambient-sourced vapor, although usually not simultaneously.

The peer-reviewed literature on the experimental hygrothermal performance of foundation insulation systems in cold climates is sparse (other than some of the references cited herein). There are studies based on simulations (for example, Chuangchild et al. [2004]), and there is a fairly extensive discussion in the *Building Foundation Design Handbook* (Labs et al. 1988) that also is not based strongly on empirical data. Specific guidance on the durability requirements for foundation wall insulation assemblies in cold climates is not included in the 2006 *International Energy Conservation Code* (ICC 2006). However, specific guidance is provided in, for example, the 2009 *Minnesota Energy Code*. In this code, novel basement wall insulation system designs that are not compliant with the "standard" prescriptive rules are required to comply with the performance option as stipulated in Section N1102.2.6.12. In particular, Section N1102.2.6.12.1 states that "The foundation shall be designed and built to have a continuous water separation plane between the interior and the exterior" (State of Minnesota 2009).

Unfortunately, the statute does not explicitly define a water separation plane (WSP).[1] However, as the statute was based on a research report prepared for the Minnesota Department of Labor and Industry (Goldberg and Huelman 2005), the definition given in the report on which the language of the performance option rules was based is:

> **Bulk water separation plane:** A single component or system of components creating a plane that prevents capillary water flow and water flow caused by hydrostatic pressure.

1. A definition of the WSP is expected to be included in the 2013 revision of the statute.

Louise F. Goldberg *is the principal of Lofrango Engineering, Minneapolis, MN.* ***Mark L. Stender*** *is president of Moisture Management, LLC, Chaska, MN.*

In a later development (discussed in Goldberg et al. [2010]), this definition was modified to the following:

> A *water separation plane* (WSP) is a single component or a system of components creating a plane that effectively resists capillary water flow and water flow caused by hydrostatic pressure and provides a water vapor permeance of 0.1 perms (5.75 ng/s.m^2.Pa) or less to retard water vapor flow by diffusion.

From a design perspective, therefore, the WSP separates the interior and exterior sides of the foundation insulation system from a water transport perspective (in all phases). Hence, condensate from water vapor originating on the exterior side (soil, ambient environment) of the WSP must be disposed of to the exterior and condensate from interior water vapor sources on the interior side. This creates a difficulty for managing interior bulk water using traditional methodologies such as an interior footing drain tile, since it is not possible to route interior condensate runoff across the WSP without perforating it in some way, nominally violating the performance rule requirement that the WSP be continuous.

The problem is exacerbated for interior foundation wall retrofit insulation systems, particularly those in applications where there is no existing interior footing drain tile and the wall experiences significant bulk water leakage. In order to reduce installation costs and, in particular, avoid the high cost of retrofitting the foundation with an interior footing drain tile, a means of routing the exterior-sourced bulk water to an interior disposal within the WSP is required. This drainage must not result in leakage of significant quantities of water vapor from vapor-saturated wall drainage cavities on either side of the WSP to the foundation interior. The drainage system should also not permit vapor transport across the WSP.

A foundation wall insulation system embodying an integrated water management system (WMS) that addresses these issues and that is compliant with the performance criteria in the *Minnesota Energy Code* has been developed, patented (Goldberg and Stender 2011a, 20llb, 2012), and tested under severe boundary conditions in a Minneapolis, Minnesota, climate. The results of the experimental research are reported herein.

THE WATER MANAGEMENT SYSTEM

The WMS as tested is shown in Figure 1. In the experiment, the base plate of the system was installed on the upper surface of an isolating stud frame base plate and sealed to this plate, the frame studs, and the masonry block wall surface.

With reference to Figure 1, the system comprises a WSP, a bulk water drainage cavity, fixtures to retain the insulation and WSP, and an interior finishing system comprising, in this case, of 2 × 2 in. (51 × 51 mm) nominal wood studs 24 in. (609 mm) on center covered with unpainted 0.5 in. (13 mm) thick gypsum board. A clear gap between the studs and the insulation surface is provided to accommodate utilities such as electrical wiring and plumbing.

Two different insulation systems were tested with the same WMS; see Figure 2, Panels A and B. In the experimental configuration, the WSP was simply a dimpled high-density polyethylene foundation waterproofing sheet with a manufacturer's reported permeance of 0.05 U.S. perms (2.86 ng/s·m^2·Pa) per ASTM Test Method E96 (2005). In the case of Panel A, with semi-rigid fiberglass board insulation, a single sheet was used with the dimples facing toward the wall. In the case of Panel B, with spray foam insulation, two sheets were laminated together so that the dimples projected outward to the interior as well as to the exterior. This was done for convenience because single-foundation waterproofing sheets with dimples protruding on both sides are quite readily available.

The water vapor sealing and bulk water transport system has two components: wicking material adhered to both sides of the bottom edge of the WSP and a pair of seals on either side of the WSP that contact the wicking layers. The WSP assembly is inserted into the receiver cavity and held in place with a retention assembly. When installed, the retention assembly causes the inboard and outboard seals to be compressed against the wicking material to the extent necessary to provide a robust water vapor seal while not impeding the flow of bulk water by capillary action through the wicking sheets.The bulk water from both sides of the WSP is collected in the receiver cavity, from which it passes into the bulk water drainage cavity via weep holes drilled at intervals through the base of the receiver cavity. In the experiment, the drainage cavities in Panels A and B were drained to interior receivers via clear plastic tubing.

When operating as intended, the WMS seals both the interior and exterior cavities on either side of the wall WSP from each other as well as from the bulk water drainage cavity. As the drainage cavity can be connected to a vapor-sealed sump, the system isolates the bulk water collection system as well as the cavities on either side of the WSP from the interior. As long as the WSP below the drainage cavity (typically the sub-slab vapor retarder) is physically adhered to the drainage cavity, the overall system meets the requirements for a continuous WSP as required by the performance option in the *Minnesota Energy Code*. Further, the WSP also meets the requirements for an air barrier (Chapter 1322, Section N1102.2.6.12.4; State of Minnesota 2009) without necessitating an additional layer.

The top plate of the WMS was designed so that the insulation, studs, and gypsum board spanning the wall surface between the top and bottom plates are aligned vertically. This configuration permits easy assembly of the insulation and interior finish components without the need for any additional components.

The top plate assembly includes a 0.75 in. (19 mm) deep channel into which a material that qualifies as a fire break (such as gypsum board) is inserted. This provides the code-required fire break above any combustible insulation (such as polystyrene or polyurethane). The WSP is inserted into the top receiver cavity that is pre-filled with a suitable sealant (such as butyl caulk) sealing the WSP on both sides as well its top edge.

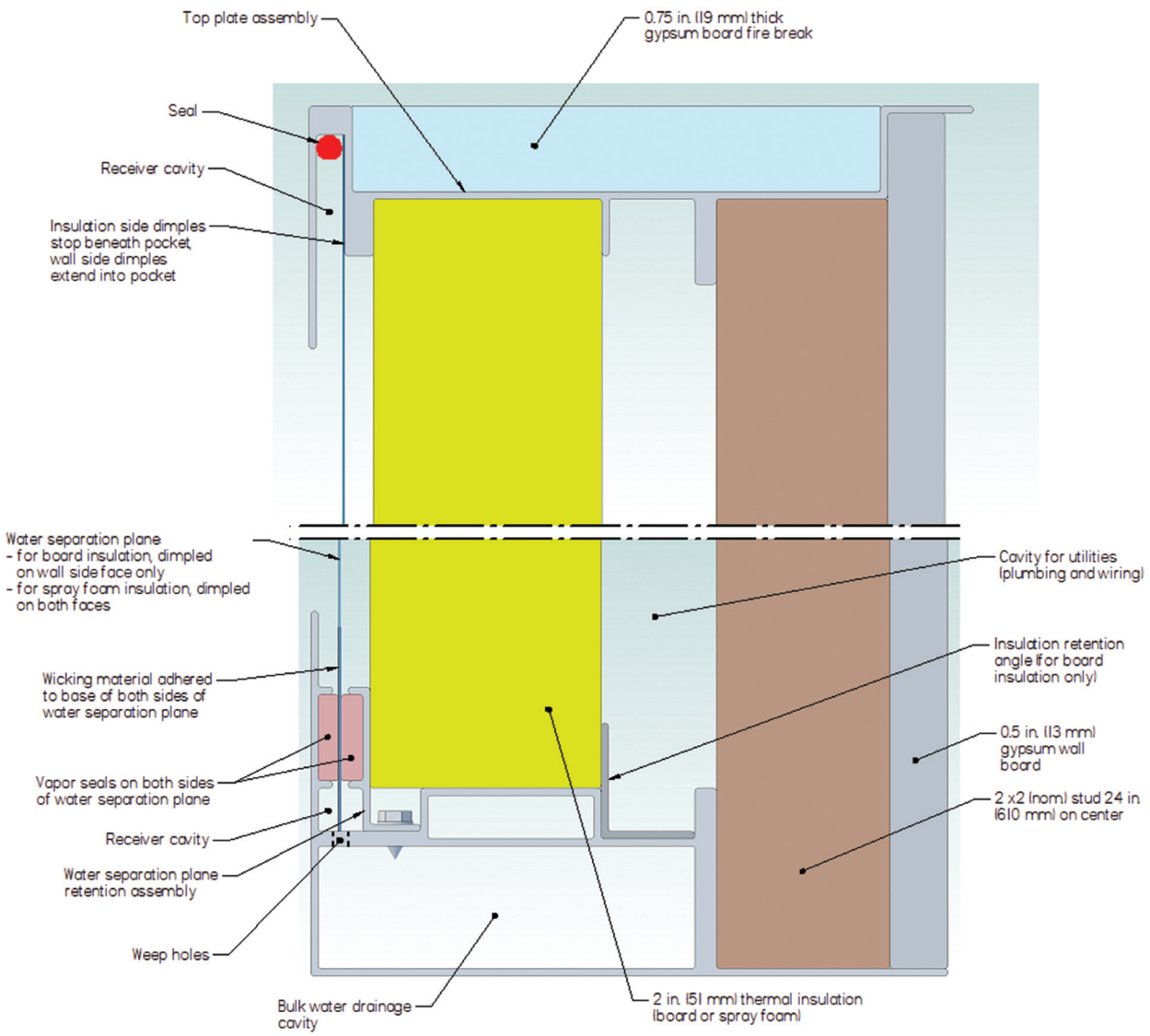

Figure 1 *Water management system (U.S. Patent nos. 8,001,736, 8,074,409 and 8,316,597).*

The only thermal bridging that occurs in the WMS assembly is through the three polyvinylchloride horizontal components of the top and bottom assemblies (each with a thickness of ~1/16 in. [1.6 mm]) and the gypsum fire break in the top plate (0.75 in. [19 mm]). With a bridging depth of about 2.5 in. (63.5 mm), the four bridging elements together yield a nominal steady-state thermal resistance (R-value) of 2.14 $ft^2 \cdot °F \cdot h/Btu$ (0.377 $m^2 \cdot K/W$). As the net thickness of the bridging elements is less than 1 in. (25.4 mm), the overall thermal bridge in the WMS is significantly less than the typical 24 in. (610 mm) on center 2 × 4 interior stud frame used to support fiberglass batt foundation wall insulation. In cases where a continuous plastic material insulation system is used (such as extruded polystyrene board), a fire break is required in any case above the insulation and is typically a 2 × 4 softwood plate. The bridging of this latter system has an R-value of 4.24 $ft^2 \cdot °F \cdot h/Btu$ (0.747 $m^2 \cdot K/W$). Thus, the net heat flow *per unit width* of the WMS thermal bridge is 0.014 Btu/ft·°F·h (0.024 W/m·K) and that of the fire break in a continuous rigid-board system is 0.029 Btu/ft·°F·h (0.051 W/m·K). The thermal bridging of the WMS is therefore less than that of a typical continuous rigid-board based insulation system.

It is important to note that the WMS tested in the experiment was not the final production version that will be fabricated from extrusions that intrinsically will yield a watertight bulk water drainage system (Figure 1).[2] Hence, of necessity, the system tested was built up from individual polyvinylchloride parts (angles, channels, and sheets) fastened together with adhesive. Thus, though every effort was made to make the bottom plate, in particular, watertight, leaks were expected to and eventually did occur over the duration of the experiment.

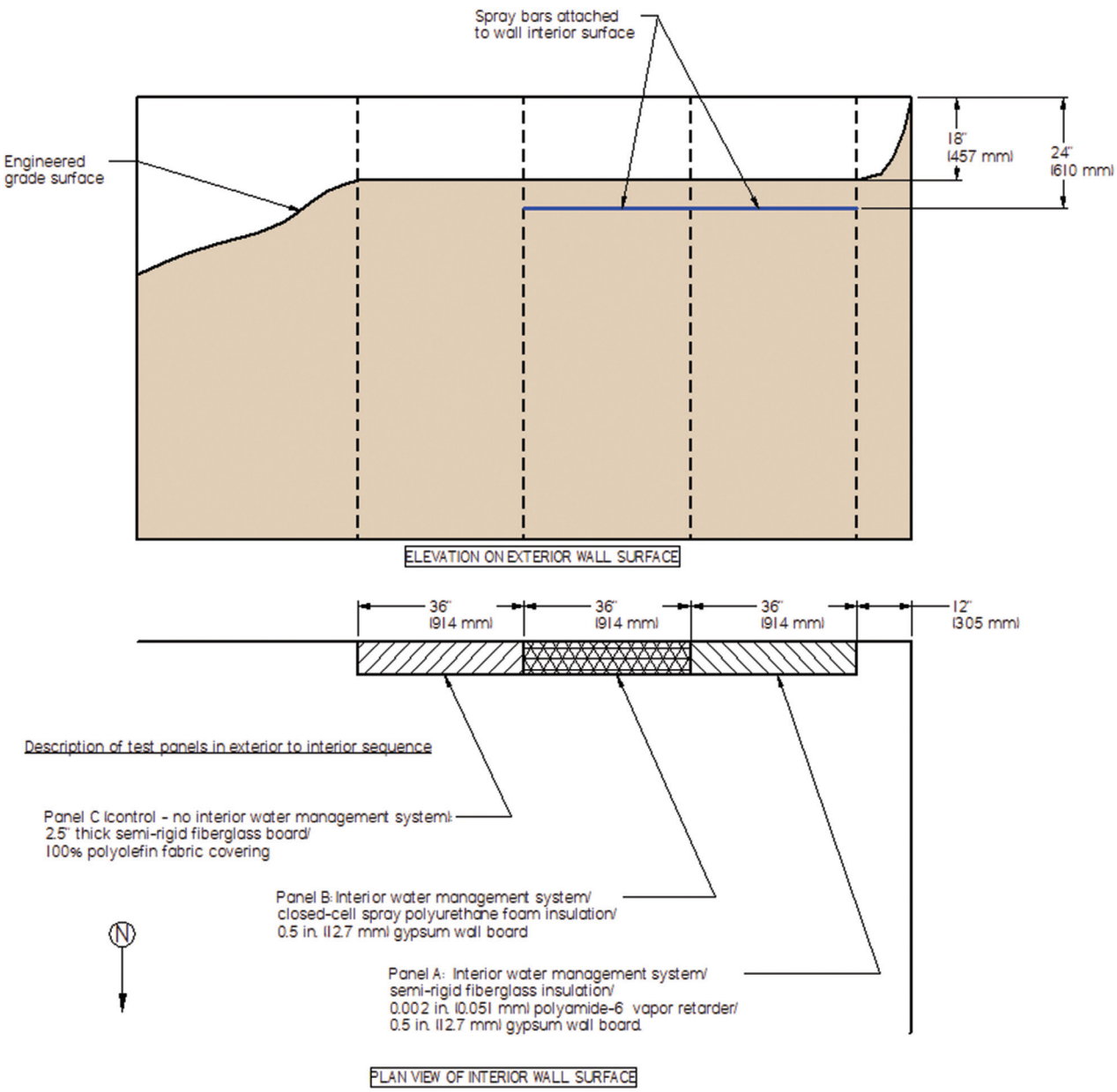

Figure 2 *Experimental schematic design.*

The observed leaks cannot occur in the production WMS fabricated from extruded components.

DESCRIPTION OF THE EXPERIMENT

The experiment was conducted in a foundations laboratory approximately 14 × 8 ft (4.3 × 2.4 m) in size located in Bloomington, Minnesota. The south and west walls were of masonry block construction fabricated from standard two-core, unfilled masonry blocks nominally 8 × 16 × 10 in. (203 × 406 × 254 mm) in size. The north and east walls were interior stud frame partition walls fitted with exterior extruded polystyrene insulation. The laboratory was in the lower level of a two-story structure and the floor joist cavities were filled with encapsulated fiberglass batt insulation. The laboratory was equipped with an electrical resistance convection heater, an air conditioner, and a steam humidifier, all of which were controlled digitally by the laboratory data acquisition and control system. A freestanding dehumidifier was introduced into the laboratory midway through the experiment with an independent digital control (that is, it was not managed by the data acquisition and control system as was the case for the other plant).

2. Extruded components were not available at the time of the experiment.

Schematic Design

The schematic design of the experiment is shown in Figure 2. The experiment comprised three test panels each 36 in. (914 mm) wide by approximately 92 in. (2.34 m) tall. Each test panel was mounted into a cavity of a stud frame located on the south wall of the laboratory. The stud frame was sealed to the wall and the floor. The rim joist cavities above the south wall were filled with closed-cell spray polyurethane foam to air-seal the top of the foundation wall and rim board. The east masonry block wall and south wall adjacent to the stud frame containing the test panels were left bare for the beginning of the experiment and then covered with 2 in. (51 mm) of extruded polystyrene insulation.

Three panels were tested as shown in Figure 3:

- Panel A consisted of the WMS mounted on the interior surface of the wall with 2 in. (51 mm) of semi-rigid fiberglass board insulation covered with a 0.002 in. (0.051 mm) thick polyamide-6 warm-side vapor retarder beneath 0.5 in. (12.7 mm) unpainted gypsum board.
- Panel B also included the interior wall surface WMS with 2 in. (51 mm) of closed-cell spray polyurethane foam insulation (with no additional warm-side vapor retarder), again beneath 0.5 in. (12.7 mm) unpainted gypsum board.
- Panel C acted as the control without a WMS, with 2.5 in. (64 mm) semi-rigid fiberglass board insulation

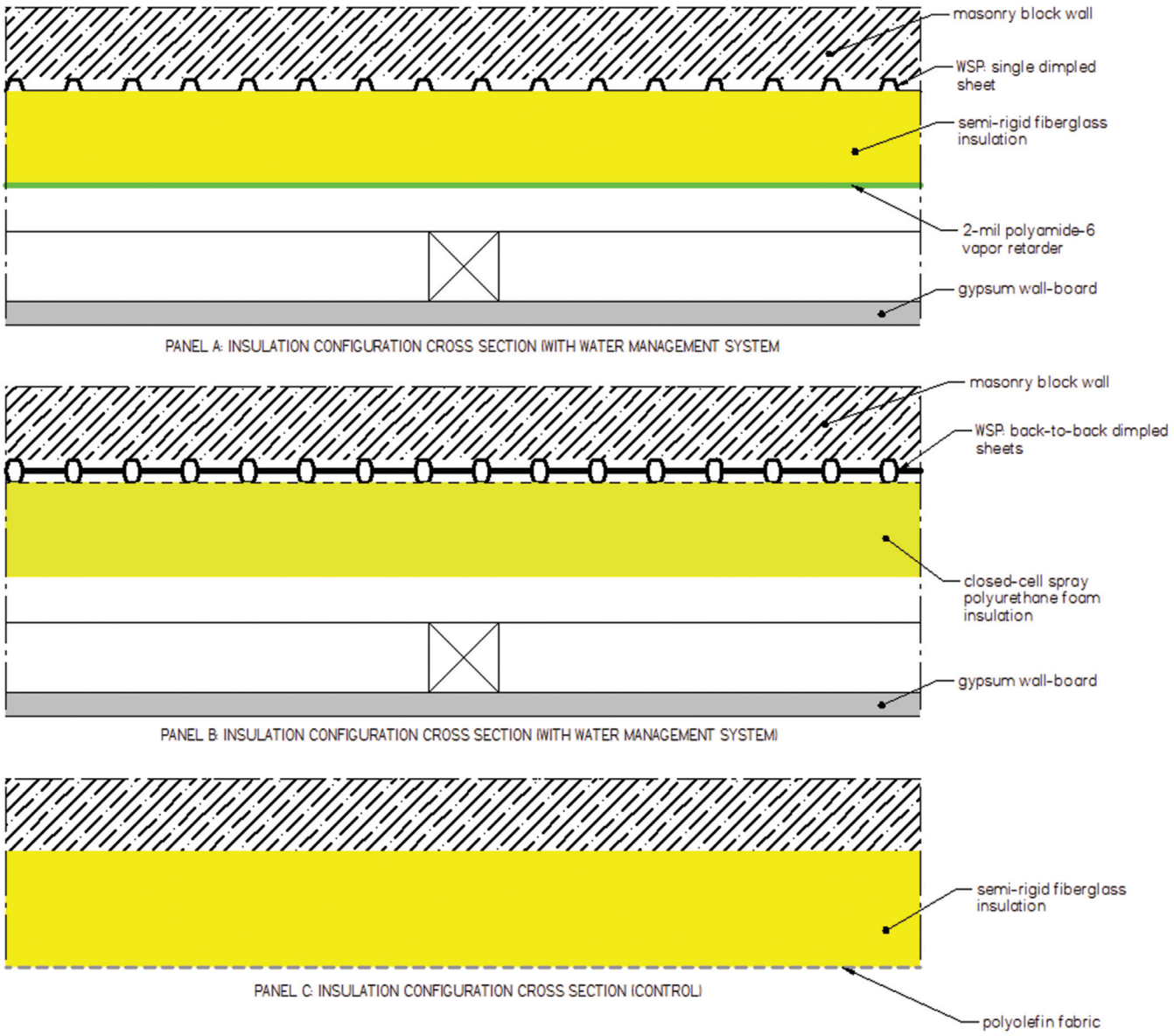

Figure 3 *Test panel insulation cross sections.*

covered with 100% polyolefin fabric on its interior surface as the finish. No warm-side vapor retarders or gypsum were installed. This system approximated a basement insulation system tested previously (Goldberg and Aloi 2001).

The primary purpose of the experiment was to test the ability of the WMS to drain bulk water from both sides of the WSP. In order to approximate bulk water leakage from the exterior, identical spray bars were mounted on the interior wall surface of Panels A and B about 24 in. (610 mm) below the top of the wall (6 in. [152 mm] below grade). These spray bars were operated in parallel in a pulsatile mode with both the water ejection period and the period between ejections being controlled independently by the laboratory data acquisition and control system so that Panels A and B received the same volume of water. As control Panel C essentially had no resistance to vapor flow from the interior, all of the condensate from the diffusion of interior humidity was absorbed into the masonry block wall or ran down to the floor.

Instrumentation

The transducer layout is described in terms of Figure 4, which is an image captured from the real-time data display system for Panel A that had the greatest number of sensors. The transducers are color-coded according to the data readout background as follows:

- Gray: relative humidity
- Blue: temperature
- Pink: masonry block moisture content (qualitative)
- Red: drainage cavity liquid level (qualitative: both indicator lights off implies dry, yellow indicator light only implies damp, yellow and red indicator lights on implies wet)

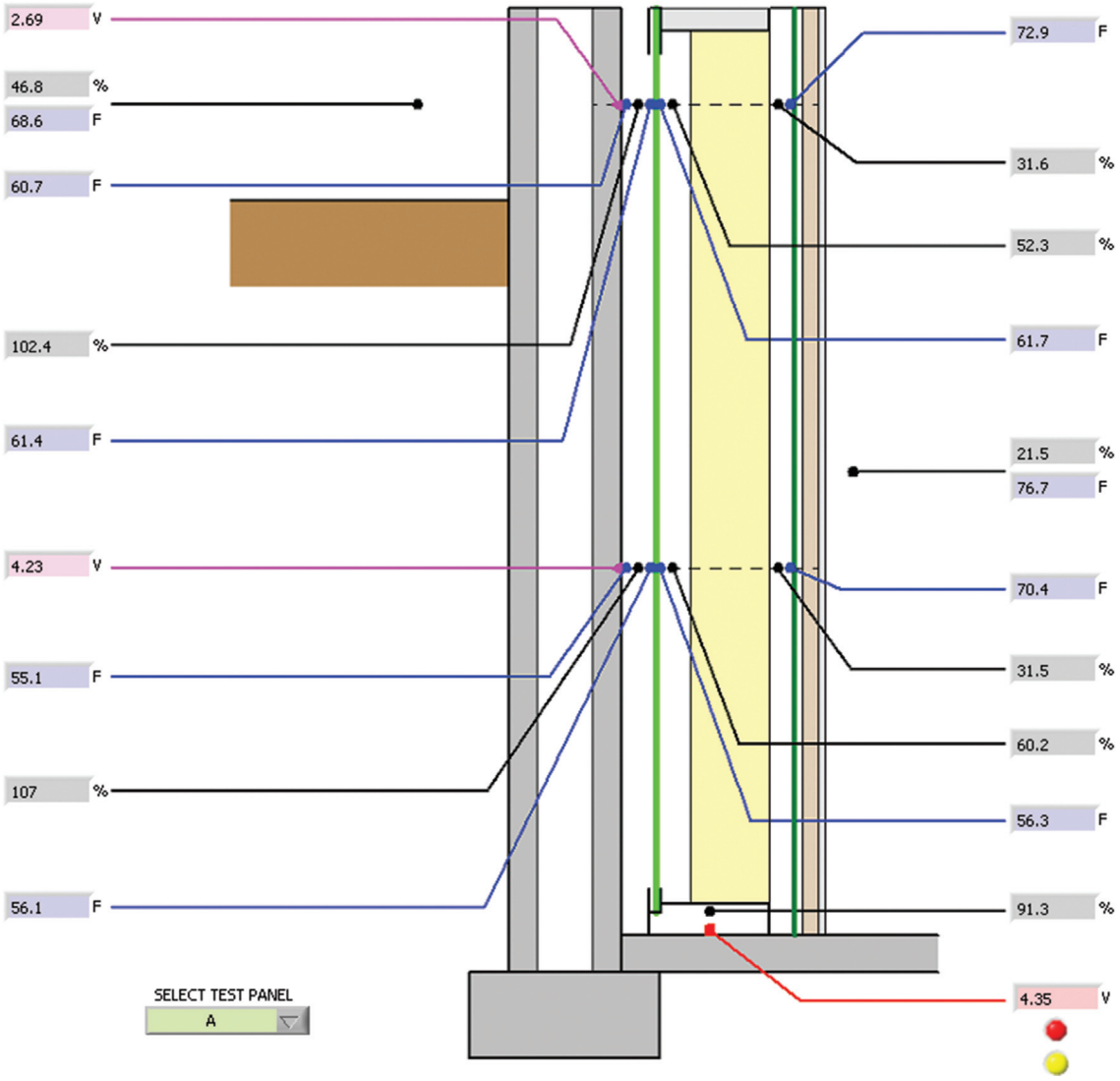

Figure 4 *Real-time data display for Panel A.*

The transducers were located at the mid-heights of the above- and below-grade wall sections, respectively, and located at the horizontal midpoint of the test cavity. The temperature and relative humidity (RH) were measured on either side of the WSP (shown schematically in Figure 4 as the lighter green vertical line between the wall and the insulation) as well as on the exterior face of the warm-side vapor retarder (shown in dark green). The drainage cavity contained a RH sensor as well as a water detector.

In addition, an experimental transducer was deployed to qualitatively assess the moisture content of the interior masonry block wall surface. The transducer sensor consisted very simply of two sheet metal screws (forming electrodes) inserted into the wall surface at a spacing of about 14 in. (356 mm) (see Figure 13). The electrodes were connected to the poles of a standard wood moisture content transmitter via a relay multiplexer. The moisture content was inversely proportional to the potential difference across the electrodes with a completely dry wall registering about 10 V. These sensors operated successfully for about the first 80% of the experimental duration but eventually failed owing to corrosion of the electrodes. This produced a galvanic corrosion cell that generated sufficient voltage to burn out the input stage of the moisture transmitter.

The exterior temperature and humidity were also measured about 8 in. (303 mm) away from the above-grade wall exterior surface as well as about 8 in. (203 mm) from the interior panel surface at the mid-wall position. The barometric pressure also was recorded.

The sensor layout for Panel B was identical to that of Panel A except, since there was no interior vapor retarder in this panel, the temperature and RH transducers between the insulation and the gypsum board were deleted. In Panel C, without a WMS, all of the transducers to the right of the light green vertical line in Figure 4 were deleted with the exception of those for interior temperature and RH.

Relative humidity was measured with individually calibrated thin-film capacitance transducers with an accuracy of ±3.5% up to about 92% RH. Above this humidity, this type of transducer becomes unreliable (note the readings above 100% adjacent to the wall in Figure 11), particularly next to materials (such as masonry blocks) exhibiting a "hockey-stick" sorption isotherm above 90% RH (a small change in RH is produced by a large change in surface moisture content). This was the motivation for deploying the experimental masonry block surface moisture content sensors even though these sensors were only capable of yielding qualitative data. The temperatures were measured exclusively with T-type (copper-constantan) thermocouples with an overall accuracy of 1.8°F (±1°C).

Data were collected continuously with a scan interval of about 3 s and were time-integrated so that a temporal average was recorded every 6 min. Data capture commenced on December 23, 2011, and continued through June 8, 2012, spanning a heating season and part of a cooling season. The raw data were post-processed to yield relevant psychrometric variables such as condensing surface dew-point temperatures and cavity vapor pressures.

Experimental Methodology

The primary purpose of the experiment was to test the bulk-water-handling capability of the WMS under very severe boundary conditions in a cold climate. The intention was to test the system to the point of failure to determine which aspects of the design required improvement or modification prior to manufacturing on a mass-production basis. Thus, the interior RH boundary condition in particular was driven to a maximum of 72% at 71°F (21.6°C) when the exterior ambient temperature was at freezing. Clearly, such severe conditions usually are not encountered in cold-climate residential basements during the heating season.[3]

Further, it was desired to test the WMS with the WSP being wetted from both sides simultaneously during the heating season. This could not be accomplished safely using the spray bars owing to the potential of water freezing in the pipes. Thus, the approach adopted was to leave the walls on either side of the test panels bare for about the first two months of the test period, allowing the high levels of interior humidity to be transported through the masonry blocks to the rear of Panels A and B. Thereafter, the bare walls were covered with 2 in. (51 mm) of extruded polystyrene insulation yielding a Class II vapor retarder with a permeance of about 0.6 perms (0.32 ng/Pa·s·m^2). This strategy was effective in producing saturated vapor conditions during the heating season on both sides of the WSP simultaneously.

Water injection using the spray bars commenced on May 14, 2012, after the laboratory interior had dried out (RH less than 24%) and proceeded until the termination of the experiment. The chosen injection rate was a 1 s pulse every two hours, corresponding roughly to a high-volume seep through the walls (test Panels A and B were wetted across their full 36 in. [914 mm] width).

The insulation systems tested were chosen to represent two of the more common approaches to foundation insulation in a cold climate with different vapor permeances and diffusion phenomenologies. Semi-rigid fiberglass board was chosen for Panel A (rather than the more conventional R-13 fiberglass batts) largely for convenience since it was easily accommodated by the experimental WMS components and has about the same vapor permeance as a batt; that is, they are both essentially vapor open. Previous research (Goldberg 2006) showed that an R-13 fiberglass batt/2-mil (0.05 mm) thick polyamide-6 warm-side vapor retarder combination yielded significant condensation on the interior foundation wall surface, thus providing a good test of the interior drainage capability of the WMS (although with asymmetric wetting/

3. The laboratory interior resembled a very wet cave with condensate dripping prodigiously from the floor joists and every metallic surface (such as the door knob).

drying performance—lower rates of wetting and higher rates of drying were produced by the relative-humidity-dependent permeance of polyamide-6). Closed-cell polyurethane foam was chosen as the alternate since it affords nominally symmetric wetting/drying performance. The 2 in. (51 mm) thickness installed yielded a permeance of about 0.76 perms (per ASTM Test Method E96 [2005][4]) according to the manufacturer's specification (a Class II vapor retarder).

Boundary Conditions

The experimental boundary conditions are shown in Figure 5. The changes in the boundary conditions may be annotated as:

4. Test method A or B is not stated.

1. **From day 0 (12/23/11) through day 35 (1/27/12):** No humidification with 68°F (20°C) interior temperature heating setpoint.
2. **From day 35 (1/27/12) through day 60 (2/21/12):** Humidification with the RH setpoint increased in steps to 72% and the temperature heating setpoint to 70°F (21°C).
3. **From day 60 (2/21/12) through day 98 (3/30/12):** No humidification with a 70°F (21°C) interior temperature heating setpoint through day 70 (3/2/12) and thereafter 68°F (20°C) (no further humidification).
4. **From day 98 (3/30/12) through day 136 (5/7/12):** Dehumidification with a 68°F (20°C) interior temperature heating setpoint through day 98 (3/30/12) and thereafter 72°F (22°C). Note the steady increase in interior temperature during this period produced by the heat

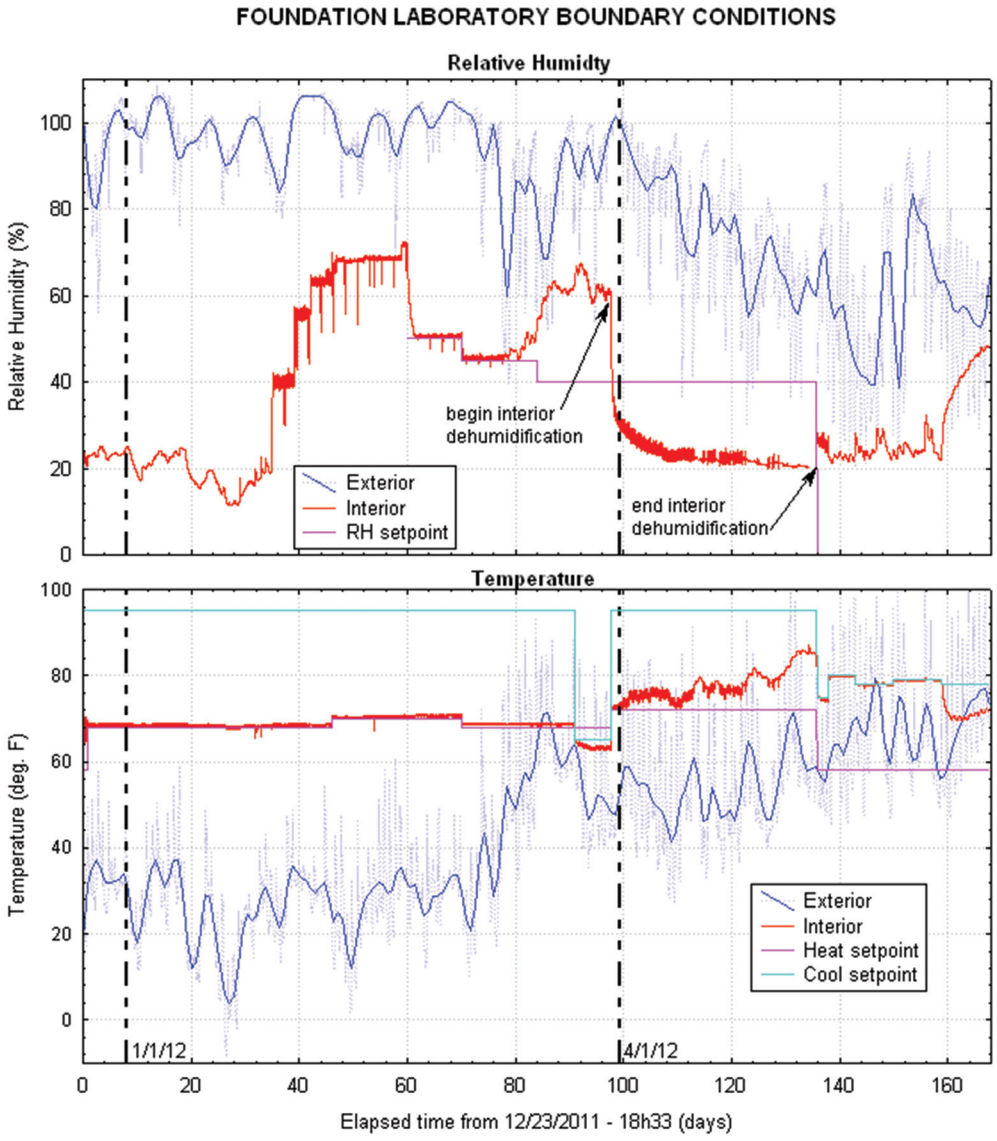

Figure 5 *Experimental boundary conditions.*

rejected to the laboratory interior by the stand-alone dehumidifier.

5. **From day 136 (5/7/12) through day 143 (5/14/12):** Air conditioning with a temperature cooling setpoint of 75°F (24°C) increasing to 80°F (27°C) on day 138 (5/9/12).
6. **From day 143 (5/14/12) through day 168 (6/8/12) (end of experiment):** Water injection at wall surface of Panels A and B (1 s pulse every 2 h) and air conditioning with a temperature cooling setpoint of 78°F (26°C).

In summary, the experiment sequence was a thermal equilibration period to provide a "normal basement" operating baseline, a period of interior humidification to wet the WSPs in Panels A and B from both sides, a drying-out period, and lastly, a cooling season operating period with interior air conditioning and bulk water injection at the wall surface in Panels A and B.

DISCUSSION OF THE EXPERIMENTAL RESULTS

Relative Humidity Phenomenology

The RH profiles for the duration of the experiment are shown in Figures 6, 7, and 8 for Panels A, B, and C, respectively. The bottom panel in each figure duplicates the RH boundary conditions for referential convenience. All the profiles are smoothed using a negative exponential curve fitting procedure, and the surface relative humidities are the actual humidities on the surface based on the adjacent cavity vapor pressure and surface temperature (and not the measured cavity relative humidities).

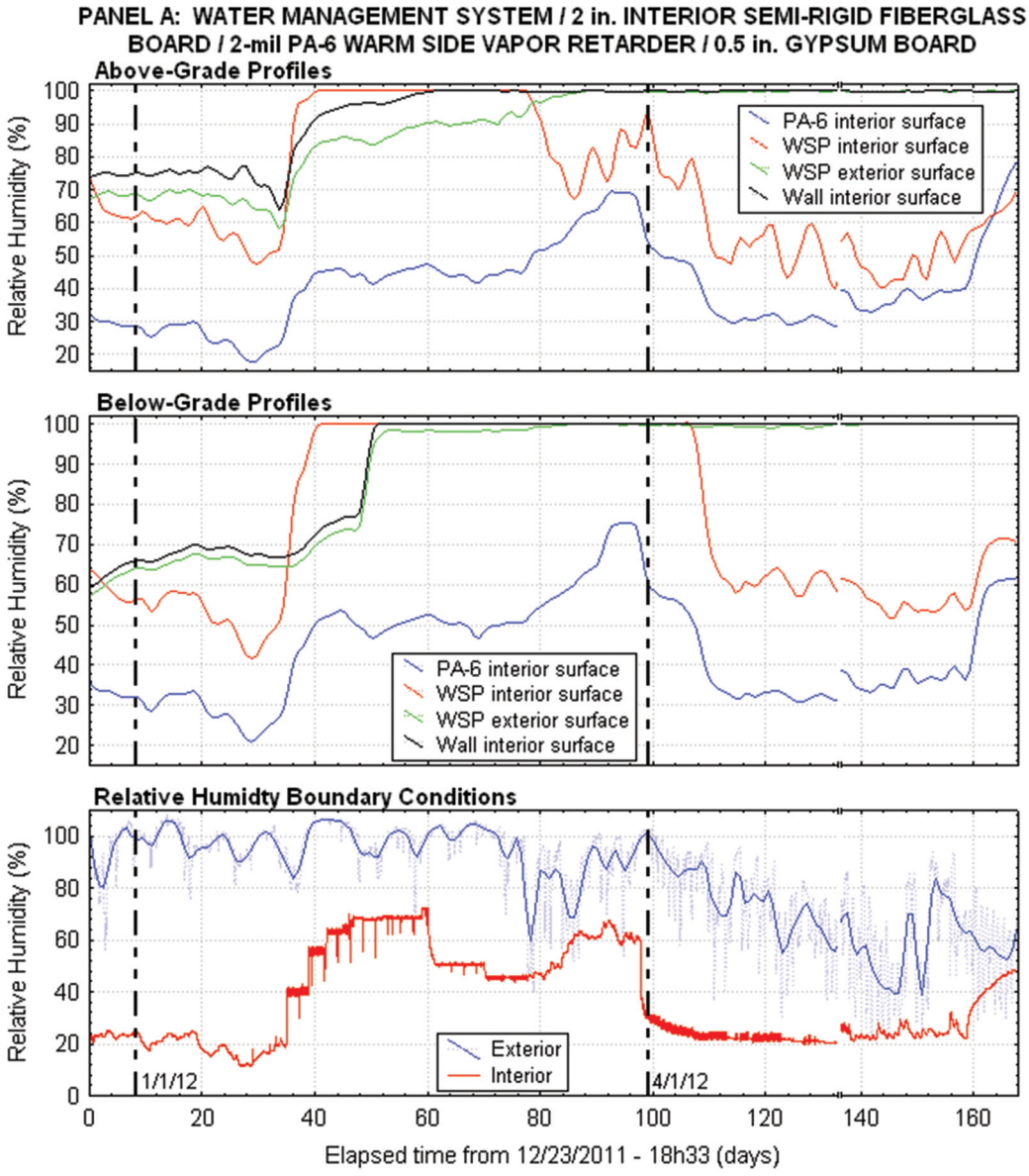

Figure 6 *Panel A relative humidity profiles.*

Figure 6 shows the sharp rise of the interior WSP RH to condensing conditions upon the start of interior humidification on day 35. Below grade, the wall and WSP exterior surface RHs reached saturation about 11 days after the WSP interior surface RHs reached saturation. Note the sharp rise in the below-grade WSP exterior's RH at about day 44, when the high-humidity incident on the bare wall adjoining Panel A reached the sensor plane by diffusion through the masonry block wall. Prior to this, the RH rise was gradual in response to soil-sourced vapor diffusion.

Above grade, the interior WSP RH increase was in phase with that below grade. But, in this case, the spike in the WSP exterior's RH occurred simultaneously with that of the interior surface RH, although after the initial spike the response was far more gradual, with the wall surface reaching saturation at day 60 and the exterior WSP surface reaching it much later at day 84. The simultaneity of the initial interior and exterior spikes is an indication of vapor leakage across the WSP at the vertical seams abutting the enclosing frame studs. The damped response of the exterior RH profiles is a consequence of a combination of freezing (diminished source strength) and drying to the exterior.

Above grade, the WSP interior surface commenced drying on day 76, while below grade this occurred much later, on day 106. The delay likely was caused by the time taken for the condensate to drain down (open surface or droplet trickle flow) to the level of the below-grade transducer as well as warmer above-grade wall surface temperatures. However, it is

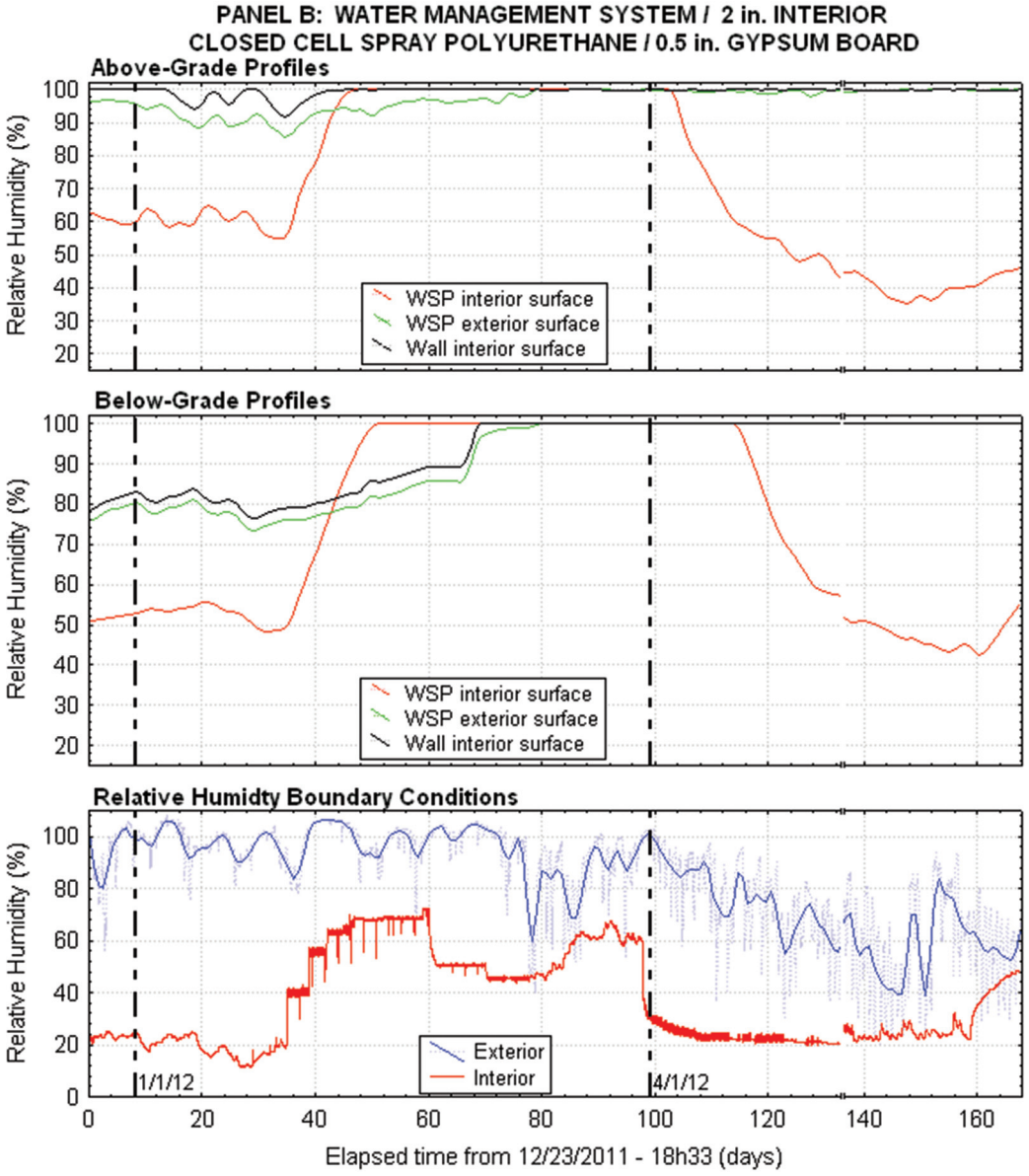

Figure 7 *Panel B relative humidity profiles.*

clear the wall surface and exterior WSP did not dry out completely. Below grade, this might be expected since bulk water injection started at day 143, but is noteworthy above grade where there was no water injection. Clearly, a risk in using non-attached interior WSPs is the creation of a perpetually wet exterior drainage cavity under the appropriate exterior boundary conditions.

Above and below grade, Figure 6 shows no condensation occurring on the exterior face of the warm-side vapor retarder, with the surface RH not exceeding 80% over the duration of the experiment. This is markedly different from the behavior observed in a previous experiment (Goldberg 2006) in which there was significant condensation on the wall side of the vapor retarder during the wall-drying phase.

Similar overall patterns are shown in Figure 7 for Panel B; however, there are some interesting divergences. First, the WSP interior RH reached saturation on days 44 and 45 at the above- and below-grade locations, respectively, compared with day 40 for Panel A. This is a consequence of the smaller effective permeance of the spray polyurethane foam in Panel B compared with that of the polyamide-6 vapor retarder in Panel A. Secondly, below grade, the RH spike on the wall and WSP exterior surfaces occurred on day 65, 21 days after it occurred in Panel A. This was doubtless a result of the vertical measurement plane in Panel B being effectively farther from the bare side walls than that of Panel A. Finally, the data show that at the beginning of the experiment the wall behind Panel B was wetter than those of either Panels A or C. Below

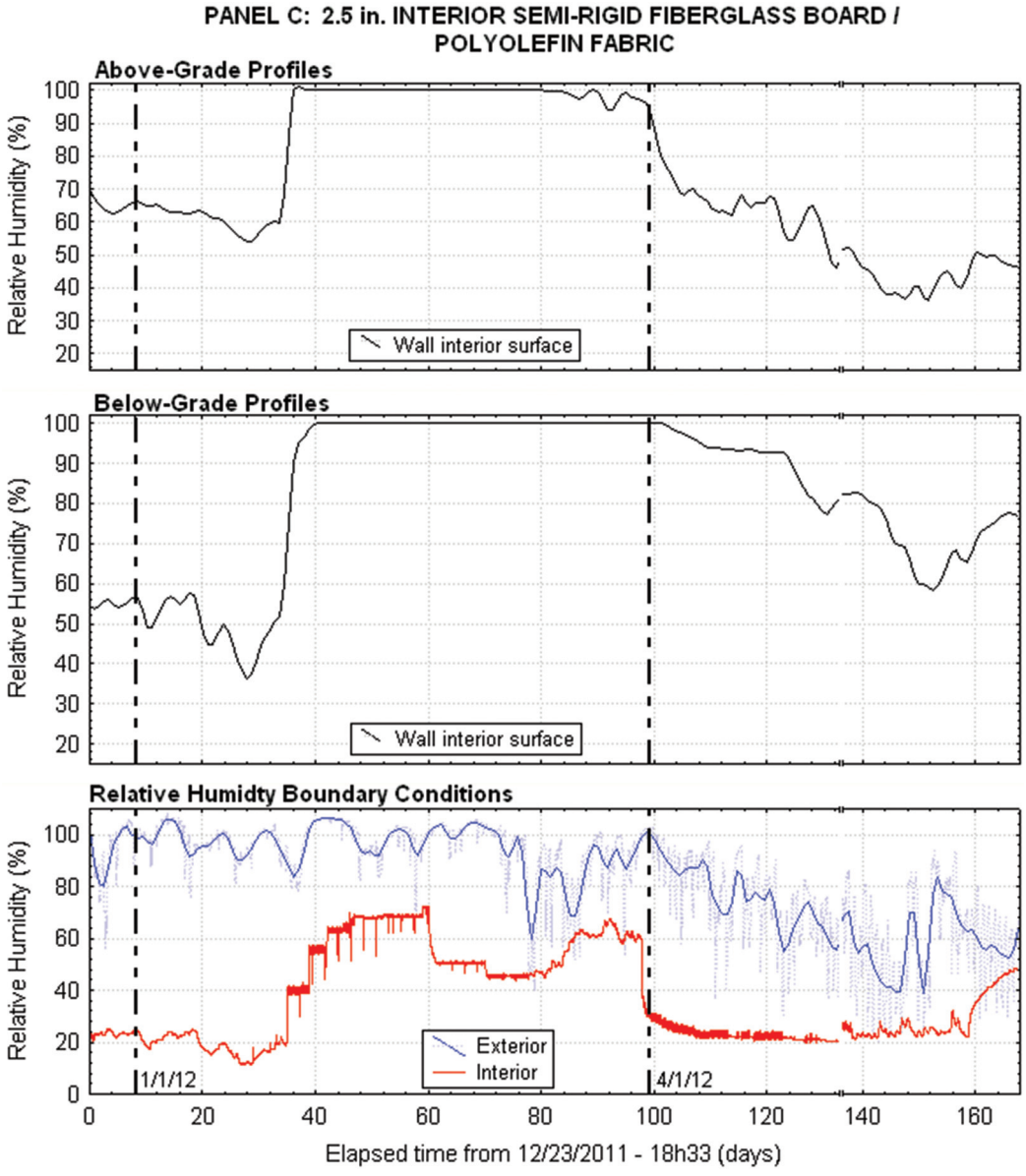

Figure 8 *Panel C relative humidity profiles.*

grade, the surface RH difference was about 20% and 25% relative to Panels A and C, respectively. Above grade, the differences were about 30%, with the above-grade wall surface already at saturation at the start of the experiment. It should be noted that data acquisition only commenced about a week after the walls were closed in, so this difference can be ascribed to edge drying effects (as there was no evidence that there were any soil moisture horizontal gradients). In other words, the drying potential to the interior from Panels A and C was larger than that of Panel B because the walls adjacent to Panels A and C were bare initially by intention. In the standard residential case where there are no bare walls around the foundation perimeter, the Panel B data would be the norm.

The above- and below-grade wall surface RH profiles in the control Panel C (Figure 8) were in conformance with previous results (Goldberg and Aloi 2001), with the wall reaching saturation on days 36 and 40 above and below grade, respectively. Comparing these results with those of Panel A in Figure 6, where the WSP interior surface reached saturation on day 40 at both locations, indicates that the polyamide-6 warm-side vapor retarder was largely ineffective (compared with no warm-side vapor retarder, as the polyolefin fabric covering Panel C was vapor open) for the applied interior boundary conditions. Thus, Panel C confirms that the condensate drainage on the WSP interior surface was as effective a condensate management strategy as the more conventional approach of using the masonry block interior surface as a heating season condensate store (Goldberg and Aloi 2001; Goldberg 2004, 2006).

Water Transport Performance

The water drainage performance of Panels A and B is shown in Figures 9 and 10. The upper two panels show the wetting/drying profiles at the below-grade location since this also captures the condensate drainage from the upper portion of the wall. The bottom panel shows the RH and wetness conditions in the bulk water drainage cavity.

For Panel A, Figure 9 shows that wetting (sensible temperature less than or equal to the dew-point temperature) began at day 46 (per Figure 6) on the exterior WSP surface, which remained wet for the duration of the experiment. On the interior surface, wetting began on day 40 and ended on day 120. In response, the drainage cavity became wet on day 52. In other words, the interior WSP surface condensate required at least six days to trickle down to the drainage cavity, indicating open surface (droplet) flow. However, the RH in the cavity stayed below 96% until after day 143, when wall-side bulk water injection began, superficially (owing to the limitations of the RH transducer discussed previously) indicating a rather small volume of condensate rundown. Of interest is that the RH only reached 100% on day 160, 17 days after the commencement of water injection. This is a strong indication that the bulk water drainage cavity was leaking, preventing any accumulation of water. This was confirmed when the experiment was dismantled (discussed in a subsequent section).

The phenomenology for Panel B as shown in Figure 10 is somewhat different. Unfortunately, the wetness sensor in the Panel B drainage trough failed at the outset of the experiment, so its data have been omitted. Wetting commenced on the exterior WSP surface on day 72 and on the interior surface at day 45. However, it is clear that as the RH in the drainage cavity remained below 76% for the entire period of the experiment prior to commencement of water injection at day 143, there was no bulk water present in the drainage cavity during this period. In comparison with Figure 9, where there was an RH of 90% or greater from day 80 onwards, this shows the following:

- Even though the exterior WSP surface reached saturation, the amount of condensate rundown on the exterior of the WSP was insufficient to wet the drainage cavity, despite the attempt to create artificially wet wall surfaces during the heating season.
- The bulk of the condensate rundown during the heating season originated from the interior side of the WSP as the volume of diffused vapor reaching the WSP from the interior in Panel A was significantly greater than that of Panel B, where it was negligible (RH peak of about 76% on day 96). This arises directly from the much lower effective permeance of the Panel B insulation system (closed-cell spray polyurethane) than that of Panel A (semi-rigid fiberglass plus polyamide-6 vapor retarder). This highlights the point that existence of saturated water vapor conditions on a vertical condensing surface does not allow inference about the quantity of condensate.

After commencement of water injection on day 143, the Panel B drainage cavity reached saturation at day 160, exactly the same behavior as in Panel A. Thus, the WMS was effective in draining the injected bulk water from the exterior drainage cavity in both Panels A and B.

Wall Surface Sorption Phenomenology

Of great interest in deploying the WMS is the wall surface moisture content. As discussed previously, RH measurements alone generally are inadequate to make inferences about the actual moisture content of the wall surface given the characteristics of masonry sorption isotherms (the "hockey stick" profile). Figure 11 shows the sorption phenomenology at the above- and below-grade locations for Panel A (the RH boundary conditions again are included for reference). Plotted are the WSP exterior *cavity* calibrated raw RH as read off the transducer and the uncalibrated voltage produced by the experimental moisture content sensor. In the case of the moisture content sensor, the moisture content is inversely proportional to the voltage with a dry condition indicated by a value of 10 V (as noted previously).

Of immediate note is that the RH transducer recorded a physically impossible RH greater than 100% at both the

above- and below-grade locations, although the extent of the over-reading (about 8% at a maximum) was much larger below grade. This simply confirms the unreliability of this type of transducer, as previously discussed, at RHs above about 92%. At the same time, the wall moisture content exhibited a gradual and stable change in response to the steeply increasing cavity RH. For example, at the above-grade location, while the cavity RH was at 100% from day 94 onward, the moisture content increased monotonically and gradually from about 3.5 V to about 1.75 V prior to the transducer failing on day 133. Similarly, below grade, after day 52 when nominal cavity saturation was reached, the moisture content sensor showed the wall surface moisture content increasing from about 6.1 V to about 3.7 V at day 88 and staying in the range from 3.7 to 4.3 V until the transducer failed on day 133.

The wall surface moisture content data show that the wall was wetter above grade than below grade, in agreement with previous experiments (Goldberg and Aloi 2001; Goldberg 2004). However, as these results are uncalibrated, any absolute inferences about the physical moisture content of the wall surface cannot be made.

Thus, in principle, these results confirm the effectiveness of the wall surface experimental moisture content measurement technique deployed to obtain a deeper understanding of the hygrothermal performance of closed drainage cavities on the interior surfaces of foundation walls.

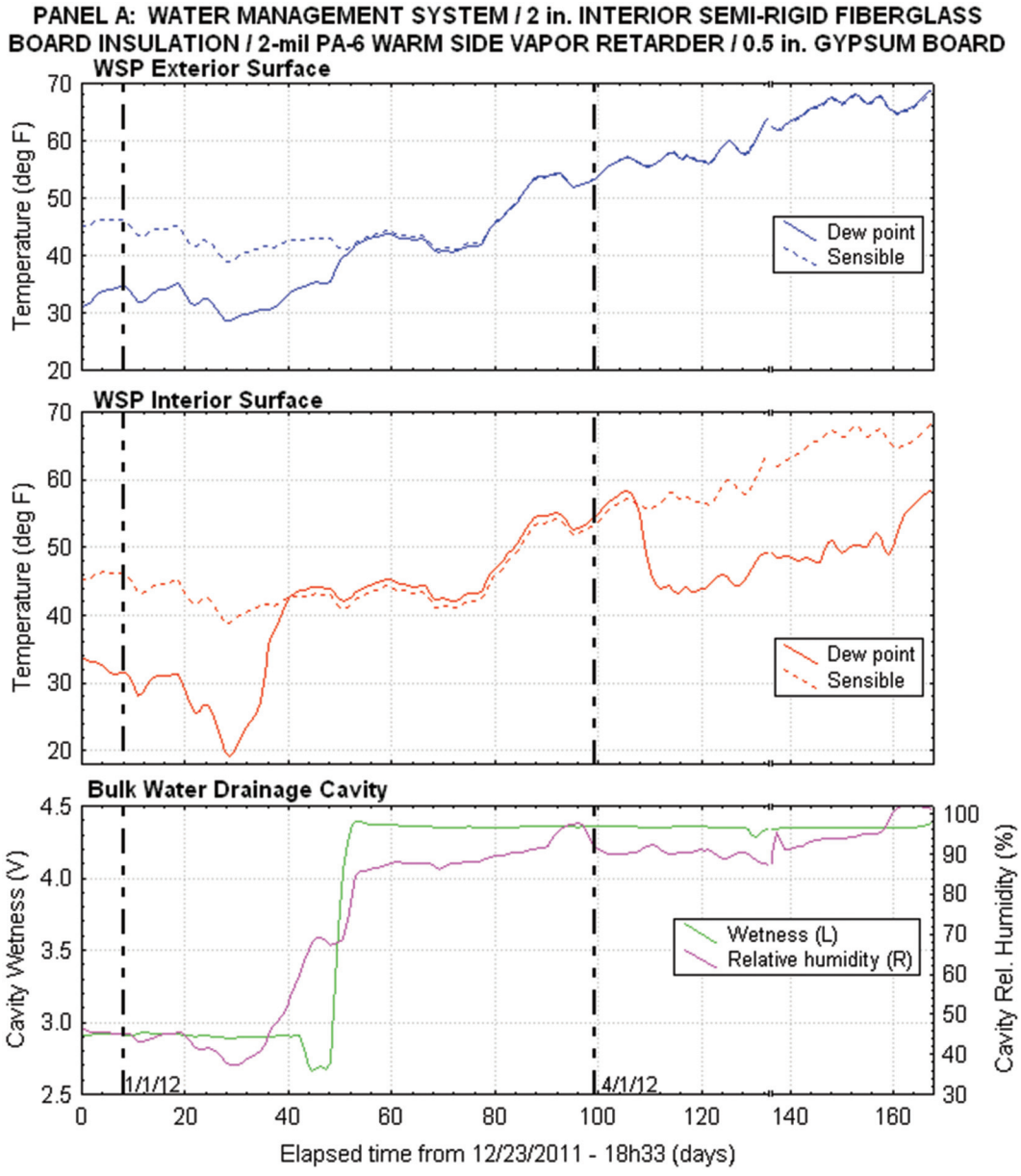

Figure 9 *Panel A below-grade water transport phenomenology.*

DISMANTLING OF THE EXPERIMENT

The experiment was dismantled on September 2, 2012, 86 days after the experiment was terminated on June 8, 2012. The long delay allowed the impact of any natural drying of the exterior wall cavity to be assessed.

The wetness of the Panel A WSP exterior wall cavity may be assessed in terms of Figure 12. This shows a partially wet wall both above and below the spray bar.

Above the level of the spray bar, there were still condensate droplets on the WSP exterior surface, but the surface was dry below the level of the spray bar, indicating that all the injected bulk water had drained away. There was no evidence of mold on either the wall or WSP surfaces.

Again, this is entirely consistent with previous experimental work (Goldberg and Aloi [2001], for example), in which insolation on the above-grade portion of a south-facing foundation wall drives moisture from the wall to the interior, where it condenses on the first condensing plane encountered.

Figure 13 shows the rear face of the WSP removed from the upper section of the wall above the spray bar in Panel B. In this case as well, the wall surface was partially wet and the rear face of the WSP was covered with condensate droplets (except for the upper part that was inserted into the top plate receiver cavity.

Thus, Figures 12 and 13 confirm that prolonged natural drying of sealed wall surface drainage cavities during the cooling season was insufficient to completely dry out these cavi-

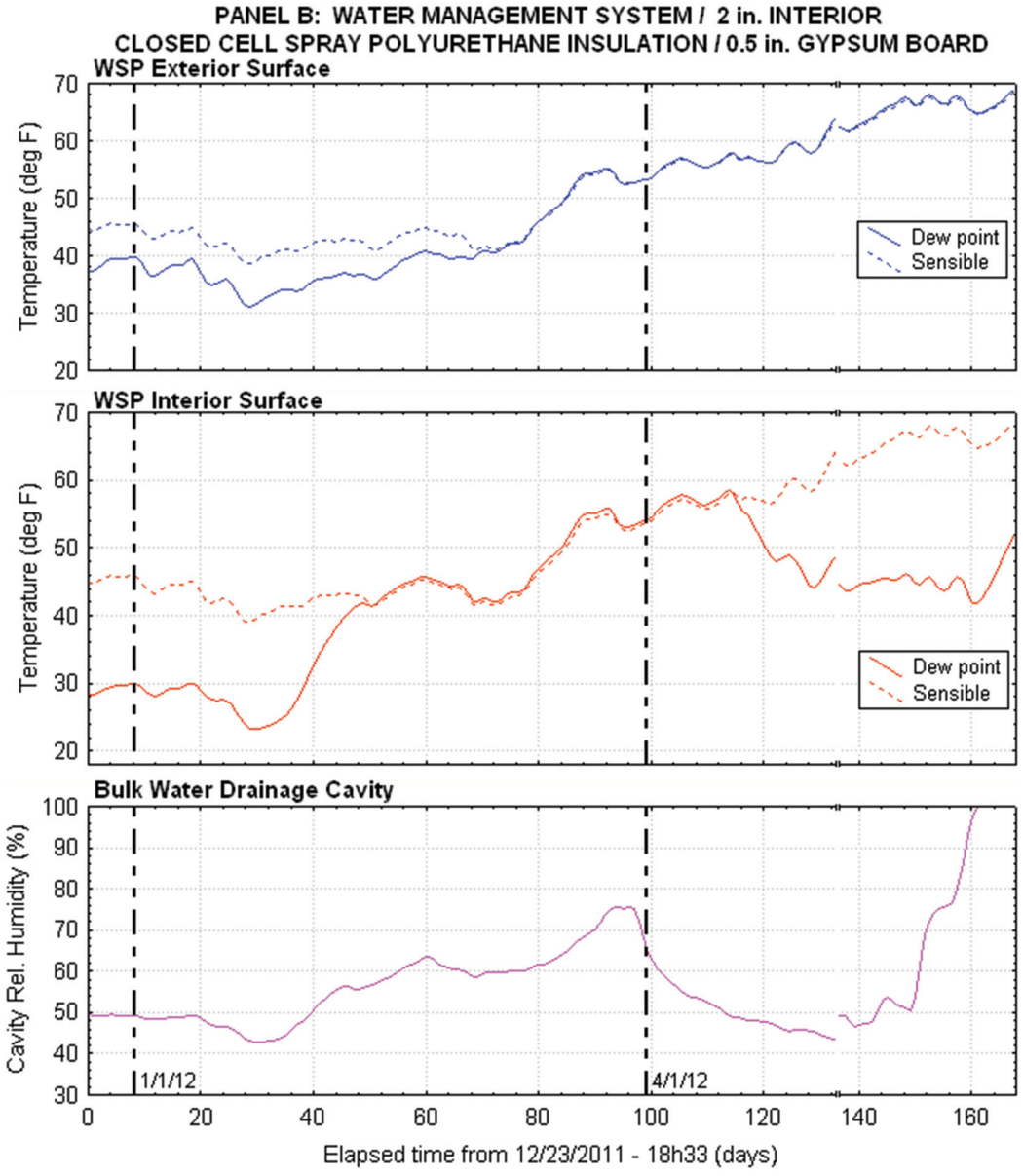

Figure 10 *Panel B below-grade water transport phenomenology.*

ties, as some residual level of moisture remains. Whether this is enough to cause mold/rot or structural problems (such as freeze/thaw-cycle-derived wall spalling) under typical basement continuous operating conditions is a question for future research. Absent such data, the possibility of a perpetually wet sealed interior wall drainage cavity must be considered in the design of foundation wall insulation systems. including the WMS tested.

Further findings during the dismantling (not shown) include the following:

- Both bulk water drainage cavities leaked where the assembly adhesive had failed (as expected).
- The caulk used to seal the WSP to the vertical studs was wet and soggy and had lost its water-sealing capacity. This accounted for the vapor leakage effects across the WSP noted in the experimental results.

CONCLUSION

The experimental results confirm that the water management system tested was effective in draining condensate from both sides of the water separation plane and bulk water from the exterior side. Attention needs to be paid to sealing the vertical edges of the water separation plane to avoid vapor bypass around these edges. Further, the results confirm that the system was in compliance with the water separation plane

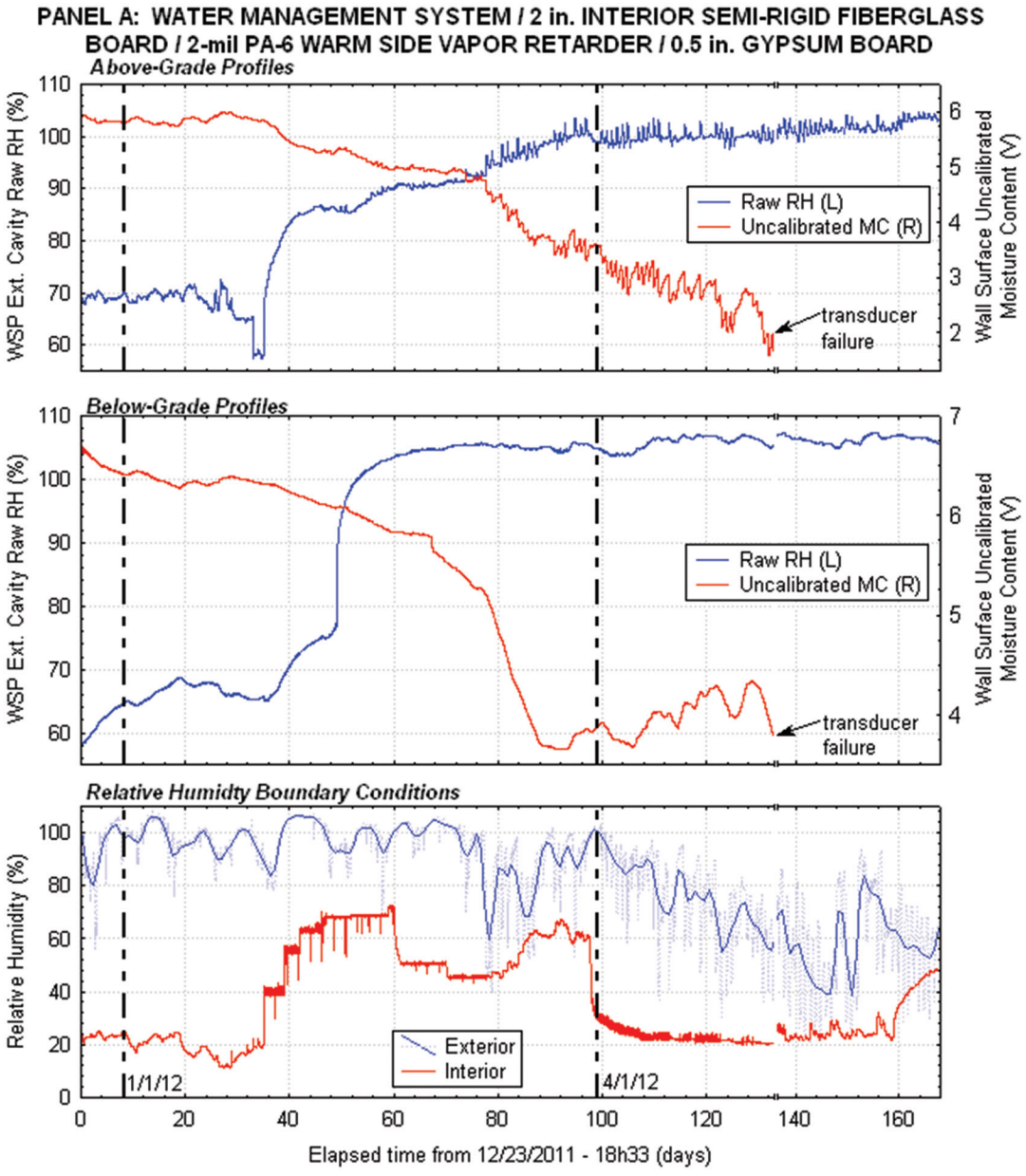

Figure 11 *Panel A wall surface sorption phenomenology.*

Figure 12 *Panel A WSP exterior cavity (dismantled on September 2, 2012).*

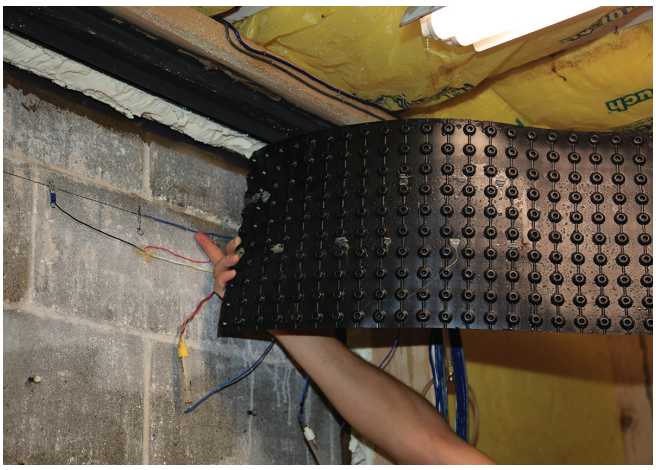

Figure 13 *Panel B WSP exterior cavity (dismantled on September 2, 2012).*

requirements of the performance option in the 2009 *Minnesota Energy Code* (State of Minnesota 2009).

Future work will include installing the production water management system (fabricated from extruded components) around the basement perimeter of a house that experiences significant bulk water leakage through the walls and monitoring the system for several years. In addition, the system will be provided to retrofit contractors for trial installations to isolate and correct any issues arising from improper installation.

REFERENCES

ASTM. 2005. ASTM Test Method E96/E 96M, *Standard Test Methods for Water Vapor Transmission of Materials*. West Conshohocken, PA: ASTM International.

Chuangchild, P., P. Ihm, and M. Krarti. 2004. Analysis of heat and moisture transfer beneath freezer foundations—Part I. *ASME Transactions, J. Solar Energy Society* 126(2):716–25.

Goldberg, L.F., and T. Aloi. 2001. Space humidity/interior basement wall insulation moisture content relationships with and without vapor retarders. *ASHRAE IAQ 2001 Conference Proceedings*.

Goldberg, L.F. 2004. Icynene foundation insulation project final report, Energy Systems Design Program Research Report, University of Minnesota, Minneapolis. www.buildingfoundation.umn.edu/IcynenFinalReport/default.htm

Goldberg, L.F., and P.H. Huelman. 2005. Minnesota Energy Code Building Foundation Rule: Amendment Proposal Development Project Final Report, Energy Systems Design Program Research Report, University of Minnesota, Minneapolis. www.buildingfoundation.umn.edu/FinalReportWWW/default.htm

Goldberg, L.F. 2006. Polyamide-6 based interior foundation insulation system: Experimental evaluation. Energy Systems Design Program Research Report, University of Minnesota, Minneapolis. www.buildingfoundation.umn.edu/CT-FTF/default.htm

Goldberg, L.F., P.H. Huelman, and S.D. Gatland II. 2010. A prototype universal building envelope hygrothermal performance standard for successful net-zero energy building design. *Proceedings of Thermal Performance of the Envelopes of Whole Buildings XI International Conference* [CD].

Goldberg, L.F,. and M.L. Stender. 2011a. Exterior Wall Assembly Including Moisture Transportation Feature. United States Patent, no. 8,001,736.

Goldberg, L.F,. and M.L. Stender. 2011b. Exterior Wall Assembly Including Moisture Removal Feature. United States Patent, no. 8,074,409.

Goldberg, L.F,. and M.L. Stender. 2012. Method of Removing Moisture from a Wall Assembly. United States Patent, no. 8,316,597.

ICC. 2006. *International Energy Conservation Code.* Section 301.1. Washington, DC: International Code Council, Inc.

Labs, K., L. Shen, J. Carmody, Y.J. Huang, R.L. Sterling, and D. Parker. 1988. *Building Foundation Design Handbook*. Minneapolis: University of Minnesota.

State of Minnesota. 2009. *Minnesota Energy Code*. MN Statutes. Residential Energy Code, Chapter 1322. Saint Paul: Department of Labor and Industry, State of Minnesota.